

# Plaquette order in a dimerized frustrated spin ladder

Ofer Shlagman and Efrat Shimshoni

*Department of Physics, Bar Ilan University, Ramat-Gan 52900, Israel*

(Received 2 July 2014; revised manuscript received 1 October 2014; published 21 November 2014)

We study the effect of dimerization (due to, e.g., spin-Peierls instability) on the phase diagram of a frustrated antiferromagnetic spin-1/2 ladder, with weak transverse and diagonal rung coupling. Our analysis focuses on a one-dimensional version of the model (i.e., a single two-leg ladder) where we consider two forms of dimerization on the legs: columnar dimers (CDs) and staggered dimers (SDs). We examine in particular the regime of parameters (corresponding to an intermediate  $XXZ$  anisotropy) in which the leg dimerization and the rung coupling terms are equally relevant. In both the CD and SD cases, we find that the effective field theory describing the system is a self-dual sine-Gordon model, which favors ordering and the opening of a gap to excitations. The order parameter, which reflects the interplay between the leg and rung dimerization interactions, represents a crystal of 4-spin plaquettes on which longitudinal and transverse dimers are in a coherent superposition. Depending on the leg dimerization mode, these plaquettes are closed or open, however both types spontaneously break reflection symmetry across the ladder. The closed plaquettes are stable, while the open plaquette order is relatively fragile and the corresponding gap may be tuned to zero under extreme conditions. We further find that a first-order transition occurs from the plaquette order to a valence bond crystal (VBC) of dimers on the legs. This suggests that in a higher-dimensional version of this system, this variety of distinct VBC states with comparable energies leads to the formation of domains. Effectively one-dimensional gapless spinon modes on domain boundaries may account for the experimental observation of spin-liquid behavior in a physical realization of the model.

DOI: [10.1103/PhysRevB.90.195143](https://doi.org/10.1103/PhysRevB.90.195143)

PACS number(s): 75.10.Pq, 75.10.Jm, 75.30.Kz

## I. INTRODUCTION

Low-dimensional quantum magnets attract a lot of experimental and theoretical attention, due to the rich physics arising from their enhanced quantum fluctuations, and competing interactions that often induce nonclassical ground states. Most prominently, quantum effects are manifested by spin- $\frac{1}{2}$  systems at one dimension. The simplest model for one-dimensional (1D) quantum antiferromagnets is the  $XXZ$  Hamiltonian, describing a spin- $\frac{1}{2}$  chain with nearest-neighbor interactions [1],

$$H = \sum_i J_{xy} (S_{i+1}^x S_i^x + S_{i+1}^y S_i^y) + J_z \sum_i S_{i+1}^z S_i^z, \quad (1)$$

where  $J_\alpha > 0$  corresponds to antiferromagnetic exchange interaction. The isotropic case  $J_{xy} = J_z$  yields the 1D Heisenberg model. This system has a nonclassical ground state at  $T = 0$  that is a gapless liquid, characterized by a lack of long-range order and power-law decay of the spin-spin correlations i.e., a critical state. The properties of this 1D liquid state at low temperatures can be evaluated in terms of gapless spin- $\frac{1}{2}$  excitations called spinons, which can be represented as interacting spinless fermions and form a Luttinger liquid.

Whether an analogous spin-liquid state can also be found in higher dimensions, and under what conditions, is an important question [2]. Typically, the 1D Luttinger liquid state is unstable to interchain couplings, which tend to favor various types of long-range order [3–7]. Therefore, a necessary condition is the presence of frustration resulting from conflict between competing interactions. A particularly interesting model for frustrated spin systems, on a 2D cubic lattice, was introduced by Nersesyan and Tsvelik [8] (NT) as a possible realization of the long-sought resonating valence bond (RVB) state [9]. The

model is described by the Hamiltonian

$$H = \sum_{j,v} \left\{ J_{\parallel} \mathbf{S}_{j,v} \cdot \mathbf{S}_{j+1,v} + \sum_{\mu=\pm 1} [J_{\perp} \mathbf{S}_{j,v} + J_d (\mathbf{S}_{j+1,v} + \mathbf{S}_{j-1,v})] \cdot \mathbf{S}_{j,v+\mu} \right\}, \quad (2)$$

where  $v$  enumerates chains and  $j$  is the site number,  $J_{\parallel}$  is the intrachain exchange constant that couples neighboring spins on the same chain, and  $J_{\perp}, J_d$  are the transverse and diagonal interchain exchange constants, respectively. The interactions of this model are presented in Fig. 1. The competition between exchange interactions on each triangle prevents antiferromagnetic ordering. The model is particularly interesting for the maximally frustrated special ratio  $J_{\perp}/J_d = 2$ , which corresponds to a critical point between two phases of valence bond crystal (VBC) [10]; i.e., a state in which pairs of spins form singlets (valence bonds) that are localized, thus forming an ordered crystal. In the anisotropic limit ( $J_{\parallel} \gg J_{\perp} = 2J_d$ ) of weakly coupled chains, the ground state at this critical point was first argued to be an RVB state [8,11]: a state where valence bonds undergo quantum fluctuations. The ground state is then a superposition of different partitionings of spins into valence bonds with no preference for any specific valence bond. However, since then it was argued that the ground state could still be a VBC [12–14].

Recently, an experimental group measured the thermodynamic properties of the material (NO) [Cu(NO<sub>3</sub>)<sub>3</sub>] (NOCuNO) [15], which appears to be a good realization of the NT model in the weak-coupling regime ( $J_{\perp} \ll J_{\parallel}$ ). NOCuNO has the unique feature that due to the symmetry of the crystal structure, its exchange interactions obey the special ratio  $J_{\perp} = 2J_d$ . Hence, it provides a suggestive realization of the model exactly

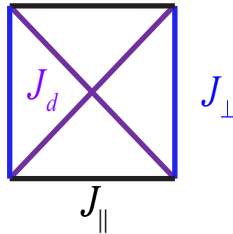


FIG. 1. (Color online) Schematic representation of the exchange interactions of the NT model.

in the quantum critical point predicted in Refs. [8,12]. The contribution to the specific heat from magnetic excitations was fitted with an empirical formula that includes a term linear in  $T$ , characteristic to gapless spinons. Susceptibility and electron-spin resonance (ESR) measurements gave no indication of long-range order throughout the whole measured temperature range, but they did indicate a considerable reduction compared to a standard spin-chain system at low  $T$ . The experimental data appear to indicate the existence of a spin-liquid component that constitutes a fraction of the degrees of freedom in the system.

A more recent study of NOCuNO by Raman scattering [16] indicated that a dynamical interplay between spin and lattice degrees of freedom exists in this material, which might lead to novel phases. Moreover, the Debye temperature in NOCuNO is of the same order of magnitude as the spin exchange interactions. It is known that when these two energy scales are comparable, the spin-lattice coupling is enhanced [17,18]. These observations motivate the study of the effect of spin-lattice coupling, which was not considered in earlier theoretical studies of the NT model.

One of the prominent consequences of spin-phonon coupling is the emergence of spin-Peierls (SP) instability. This effect occurs when the exchange couplings are modulated due to distortions in the distance between neighboring atoms, yielding an alternation of strong and weak bonds. The SP instability tends to dimerize the spin-chain, therefore it can destroy the gapless liquid state and form a VBC of longitudinal dimers [20,21]. Away from the critical point of Ref. [8] ( $J_{\perp} = 2J_d$ ), a competition arises between the SP instability (which tends to create longitudinal dimers) and the transverse exchange coupling (which tends to create transverse dimers). This competition may lead to a phase transition between different types of dimer crystals, or it may induce a new phase.

In one of the earlier theoretical works on the NT model [12], Starykh and Balents considered a dimer-dimer interaction term that may be generated by higher-order interchain interactions, and they studied the influence of this interaction term via a renormalization-group (RG) approach. They showed that various ordered nonmagnetic phases (i.e., with zero magnetization) can form even in the absence of an explicit dimerization term. The possible phases are two types of VBC, of staggered and columnar longitudinal singlets, in addition to the rung singlets and rung triplets (Haldane phase [19]) VBC states predicted by NT. Later numerical studies [13] confirmed the emergence of such phases for sufficiently strong interchain interactions. This suggests an additional mechanism for dimerization besides interaction with phonons.



FIG. 2. (Color online) Two possible ordering of valence bonds on two noninteracting chains: (a) columnar dimers (CDs), (b) staggered dimers (SDs). Thick red lines represent dimers on the stronger bonds.

A number of theoretical studies have also considered the effect of an explicit dimerization term on the Heisenberg spin-ladder without frustrating (diagonal) interactions [20–26]. Interestingly, these works found that although a dimerization term opens a gap when added to a gapless spin chain, adding such a term to a gapped spin ladder can lead to a gapless phase for suitably tuned dimerization and exchange couplings. It should be noted that the possible phases depend crucially on the relative configuration of dimers on different legs of the ladder. Specifically in a two-leg ladder, there are two distinct configurations that differ by the relative sign of the dimerization on the two chains, and they are dubbed columnar dimers (CDs) and staggered dimers (SDs) (see Fig. 2). The above-mentioned works primarily examined the SD case in spin-1/2 Heisenberg ladders, which have been found [23,24] to support massless spin excitations for sufficiently strong rung coupling. More recent studies considered the CD configuration along with the previously studied SD dimerization [27–29], finding that the ground state of the CD state is lower in energy and is always gapped.

In this paper, motivated by the experimental study of Ref. [16], we examine the effect of leg-dimerization perturbations on the low-energy physics of an anisotropic generalization of the NT model. For this purpose, we consider a two-leg ladder version of the NT model where we introduce dimerization terms on the legs as well as XXZ anisotropy of all exchange couplings  $J_{\parallel}, J_{\perp}, J_d$ . In contrast with the earlier studies [20–29], which consider the SU(2)-symmetric Heisenberg limit, we focus in particular on the case of an intermediate XXZ anisotropy ( $J_{\parallel}^z/J_{\parallel} \sim 0.6$ ), where the rung and leg dimerization terms have an approximately equal scaling dimension, and hence they compete strongly. We consider both dimerization patterns (CDs and SDs) depicted in Fig. 2: assuming the dimerization originates from a SP instability, the choice between them is dictated by the lattice deformation associated with the coupling to a certain phonon mode. Considering all the interactions (perpendicular, diagonal, and leg dimerization) in a bosonization description, we map the model onto an effective self-dual sine-Gordon model, which we show is equivalent to a spin chain in a staggered and tilted magnetic field. Our main result is that the effect of the leg dimerization on the NT model may lead to a “plaquette-ordered” state: a crystal of four-spin plaquettes where on each plaquette there is a coherent superposition of longitudinal and transverse dimers, in a configuration that breaks reflection symmetry across the ladder. There are two types of plaquette ground states corresponding to the two types of dimerized patterns CDs and

SDs. Generically, in both cases the ground state is gapped. The tuning of parameters [the dimerization  $\delta J_{\parallel}$ , the interleg coupling  $(J_{\perp} - 2J_d)$ , and the anisotropies  $J_{\alpha}^z/J_{\alpha}^{xy}$ ] leads to a smooth interpolation between longitudinal and transverse VBC (each being recovered in the appropriate limit case), without a second-order phase transition. Similarly to Chitov *et al.* (Ref. [28]), we find that the gap is larger in the CD case, hence the plaquette order in this case is more stable. Moreover, for the SD case [Fig. 2(b)], a 1D gapless (critical) state can apparently be recovered under extreme conditions: strong anisotropy of  $J_{\perp}, J_d$ , and rung exchange of the order of magnitude of the leg exchange. However, the closing of a gap in the plaquette-ordered state is always preempted by a *first-order* transition to the original VBC of leg dimers.

The paper is organized as follows: In Sec. II, we derive the low-energy model for the spin system in terms of bosonic fields. In Sec. III, we analyze the model and demonstrate the emergence of the plaquette order (Sec. III A) and the phase transition to the VBC state (Sec. III B). Technical details of the fermionization method and of the calculations of dimer correlation functions are discussed in Appendixes A and B, respectively. Finally, in Sec. IV, we summarize the results and discuss their possible relevance to the behavior of the 2D realizations of the frustrated coupled chains model.

## II. THE MODEL

We consider a two-leg XXZ ladder version of the NT model [Eq. (2)],

$$H_{\text{ladder}} = \sum_j \left\{ \sum_{\nu=1,2} \left\{ \frac{J_{\parallel}}{2} [S_{j,\nu}^+ S_{j+1,\nu}^- + \text{H.c.}] + J_{\parallel}^z S_{j,\nu}^z S_{j+1,\nu}^z \right\} + \frac{J_{\perp}}{2} [S_{j,1}^+ S_{j,2}^- + \text{H.c.}] + J_{\perp}^z S_{j,1}^z S_{j,2}^z + \frac{J_d}{2} [S_{j,1}^+ (S_{j+1,2}^- + S_{j-1,2}^-) + \text{H.c.}] + J_d^z S_{j,1}^z (S_{j+1,2}^z + S_{j-1,2}^z) \right\}, \quad (3)$$

with strong intrachain coupling ( $J_{\parallel} \gg J_{\perp}, J_d$ ) and where all exchange couplings are positive. We then introduce a dimerization term along the legs of the ladder (e.g., due to spin-Peierls instability), described by a contribution to the Hamiltonian of the form

$$H_P^{\sigma} = \frac{\delta J_{\parallel}^{xy}}{2} \sum_j (-)^j [S_{j,1}^+ S_{j+1,1}^- + \sigma S_{j,2}^+ S_{j+1,2}^- + \text{H.c.}] + \delta J_{\parallel}^z \sum_j (-)^j [S_{j,1}^z S_{j+1,1}^z + \sigma S_{j,2}^z S_{j+1,2}^z]. \quad (4)$$

This term describes a static deformation of the exchange constants along the legs. In the absence of transverse coupling between the chains 1 and 2, the ground state of each chain is a product of singlets on the strong bonds (i.e., a one-dimensional VBC), with a gap of the order of  $\delta J_{\parallel}$  between the singlet ground state and the lowest triplet excitation. The parameter  $\sigma = \pm$  is the relative sign of the dimerization on the two chains.

The leg dimerization term is relevant as long as we are away from the ferromagnetic transition point, therefore, in our case, it is strongly relevant and tends to open a gap on each chain independently. As a result, in the case of two uncoupled chains there are two possible patterns in which a VBC can form on the chains, depending on  $\sigma$ :  $\sigma = +$  yields a columnar dimers state and  $\sigma = -$  a staggered dimers state, as shown in Fig. 2.

To derive the low-energy model of the system, we first use the Jordan-Wigner transformation, which maps the spin operators into fermion fields. In the absence of magnetic field, the Fermi energy is at the middle of the band, and the fermion operators can be expressed in terms of bosonic ones related to the Fermion density fluctuations:

$$\psi_{R/L,\nu} = \frac{1}{\sqrt{2\pi a}} e^{-i(\pm\phi_{\nu} - \theta_{\nu})}, \quad (5)$$

where  $R, L$  stands for right- and left-moving fermions, respectively,  $a$  is the lattice constant, and  $\nu = 1, 2$  is the leg index. This procedure can be summarized briefly by the following spin-to-boson transformation:

$$S_{\nu}^+(x) = \frac{e^{-i\theta_{\nu}(x)}}{\sqrt{2\pi a}} \{(-)^x + \cos[2\phi_{\nu}(x)]\},$$

$$S_{\nu}^z(x) = -\frac{1}{\pi} \partial_x \phi_{\nu}(x) + \frac{(-)^x}{\pi a} \cos[2\phi_{\nu}(x)]. \quad (6)$$

We now bosonize the Hamiltonian  $H = H_{\text{ladder}} + H_P^{\sigma}$ , starting from

$$H_{\text{ladder}} = \int dx \sum_{\nu=1,2} \frac{u}{2\pi} \left[ \frac{1}{K} (\partial_x \phi_{\nu})^2 + K (\partial_x \theta_{\nu})^2 \right] + \int dx \left[ \frac{g}{(2\pi a)^2} \cos(\theta_1 - \theta_2) + \frac{g^z}{(2\pi a)^2} \cos[2(\phi_1 - \phi_2)] + \frac{g^z}{(2\pi a)^2} \cos[2(\phi_1 + \phi_2)] \right] + (J_{\perp}^z + 2J_d^z) a \int dx \frac{\partial_x \phi_1 \partial_x \phi_2}{\pi^2},$$

$$g \equiv \frac{2\pi a (J_{\perp} - 2J_d)}{(2\pi a)^2}, \quad g^z \equiv \frac{2\pi a (J_{\perp}^z - 2J_d^z)}{(2\pi a)^2}. \quad (7)$$

Here  $u$  and  $K$  are the Luttinger parameters of each chain on its own and are given by [32]

$$u = \frac{J_{\parallel}}{2} \frac{\sqrt{1 - (J_{\parallel}^z/J_{\parallel})^2}}{1 + \frac{1}{\pi} \arccos(-J_{\parallel}^z/J_{\parallel})},$$

$$K = \frac{\pi}{2 \arccos(-J_{\parallel}^z/J_{\parallel})}. \quad (8)$$

Note that the frustrating interactions  $J_d$  and  $J_d^z$  enable the tuning of  $g$  and  $g^z$  independently of each other, and make them relatively small. This consequence of the frustration is important for our discussion since different phases may appear as a function of the ratio  $g/g^z$ .

Equation (7) can be written more conveniently in terms of independent symmetric and antisymmetric modes [30–32],

$$\phi_{s/a} = \frac{\phi_1 \pm \phi_2}{\sqrt{2}}, \quad \theta_{s/a} = \frac{\theta_1 \pm \theta_2}{\sqrt{2}}. \quad (9)$$

Then,  $H_{\text{ladder}}$  assumes the form

$$H_{\text{ladder}} = \int dx \left\{ \sum_{\mu=a,s} \frac{u_\mu}{2\pi} \left[ \frac{1}{K_\mu} (\partial_x \phi_\mu)^2 + K_\mu (\partial_x \theta_\mu)^2 \right] + g \cos(\sqrt{2}\theta_a) + g^z \cos(\sqrt{8}\phi_a) + g^z \cos(\sqrt{8}\phi_s) \right\}, \quad (10)$$

where for  $J_\perp, J_d \ll J_\parallel$ ,

$$\begin{aligned} K_{a,s} &\cong K [1 \pm \gamma], \\ u_{a,s} &\cong u [1 \mp \gamma], \\ \gamma &\equiv \frac{K(J_\perp^z + 2J_d^z)a}{2\pi u}. \end{aligned} \quad (11)$$

In ladders with antiferromagnetic legs where the XXZ anisotropy is anywhere in the range between the Heisenberg and XX limits (such that  $1/2 \leq K \leq 1$ ), both sectors  $s$  and  $a$  are gapped. The nature of the resulting phase depends on the sign of  $g, g^z$ : a negative sign (i.e., effectively ferromagnetic rung coupling) yields the Haldane phase, while a positive sign (effectively antiferromagnetic rung coupling) yields a crystal of rung singlets [30–32].

Bosonization of  $H_P^\sigma$  (see, e.g., Ref. [32] for a detailed derivation) yields a term more conveniently written in terms of the original fields  $\phi_1, \phi_2$ :

$$\begin{aligned} H_P^\sigma &\sim g_P \int dx [\sin(2\phi_1) + \sigma \sin(2\phi_2)], \\ g_P &\equiv \frac{\delta J_\parallel}{\pi a}. \end{aligned} \quad (12)$$

Then, substituting Eq. (9) into Eq. (12) recasts  $H_P^\sigma$  as a coupling term between the  $a$  and  $s$  sectors. The resulting full Hamiltonian is

$$\begin{aligned} H &= H_{\text{ladder}} + H_P^\sigma = H_a + H_s + H_{as}^\sigma, \\ H_a &= \frac{u_a}{2\pi} \int dx \left[ \frac{1}{K_a} (\partial_x \phi_a)^2 + K_a (\partial_x \theta_a)^2 \right] \\ &\quad + g \int dx \cos(\sqrt{2}\theta_a) + g^z \int dx \cos(\sqrt{8}\phi_a), \\ H_s &= \frac{u_s}{2\pi} \int dx \left[ \frac{1}{K_s} (\partial_x \phi_s)^2 + K_s (\partial_x \theta_s)^2 \right] \\ &\quad + g^z \int dx \cos(\sqrt{8}\phi_s), \\ H_{as}^\sigma &= g_P \int dx \{ \sin[\sqrt{2}(\phi_s + \phi_a)] + \sigma \sin[\sqrt{2}(\phi_s - \phi_a)] \}. \end{aligned} \quad (13)$$

Note that at the critical point of the NT model, which for anisotropic rung coupling requires both  $J_\perp = 2J_d$  and  $J_\perp^z = 2J_d^z$ , the coefficients  $g, g^z$  in Eq. (13) vanish. However, away from the critical point we must consider the competition

between all the cosine terms appearing. The relevance of the terms is determined by the scaling dimensions. Let us denote by  $d_{a/s}^z$  the scaling dimensions of the terms  $g^z \cos(\sqrt{8}\phi_{a/s})$ , respectively, in the  $a/s$  sector,  $d$  of the term with coefficient  $g$ , and  $d_P$  the scaling dimension of the term with coefficient  $g_P$ . Employing a perturbative RG, these scaling dimensions are given by

$$d = \frac{1}{2K_a}, \quad d_a^z = 2K_a, \quad d_P = \frac{1}{2}(K_a + K_s), \quad d_s^z = 2K_s. \quad (14)$$

Since  $\gamma$  [Eq. (11)] is positive,  $d_s^z < d_a^z$ . Therefore,  $g^z \cos(\sqrt{8}\phi_a)$  is always the least relevant term, and it will be neglected henceforth. Comparing  $d_P$  and  $d_s^z$ , we find that for weak rung coupling ( $\gamma < 1/2$ ), the  $g_P$  term is also more relevant than the  $g^z \cos(\sqrt{8}\phi_s)$  term. This analysis of the scaling dimensions leads to the conclusion that for weak rung coupling, the dominant terms that govern the low-energy description are the  $g$  and  $g_P$  terms, which indicate a potential competition between the leg dimerization and the rung coupling (which tends to form rung dimers for  $g > 0$ ). There is a special value of  $K$  for which the scaling dimensions of the most relevant terms are equal: from Eqs. (11) and (14), we find  $d = d_P$  for

$$K^* = \frac{1}{\sqrt{2(1+\gamma)}} \cong \frac{1}{\sqrt{2}}. \quad (15)$$

For this value of  $K$  [which corresponds to an intermediate anisotropy  $J_\parallel^z/J_\parallel \approx 0.6$ ; see Eq. (8)], the competition between the leg and rung dimerization terms is maximal. In the remainder of the paper, we therefore focus our attention primarily on the regime of parameters where  $K \sim K^*$ .

We now recall that for arbitrary  $K$  in the regime of interest  $1/2 \leq K < 1$  (i.e.,  $0 < J_\parallel^z \leq J_\parallel$ , and in particular for  $K \sim K^*$ ),  $K_s < 1$ . Hence the term  $g^z \cos(\sqrt{8}\phi_s)$  is also relevant, and it tends to lock the value of the symmetric field  $\phi_s$ . This affects the interaction term  $H_{as}^\sigma$ , which has a different form for SD ( $\sigma = -$ ) and CD ( $\sigma = +$ ) configurations:

$$\begin{aligned} H_{as}^+ &= 2g_P \int dx \sin(\sqrt{2}\phi_s) \cos(\sqrt{2}\phi_a), \\ H_{as}^- &= 2g_P \int dx \cos(\sqrt{2}\phi_s) \sin(\sqrt{2}\phi_a). \end{aligned} \quad (16)$$

In a semiclassical approximation, the  $\cos(\sqrt{8}\phi_s)$  term in Eq. (13) obtains a finite expectation value that minimizes  $H_s$ . This depends on the sign of  $g^z$ : for  $g^z > 0$ ,

$$\langle \cos(\sqrt{8}\phi_s) \rangle \cong -1 \Rightarrow \sqrt{2}\langle \phi_s \rangle \cong \pi/2 \quad (17)$$

while for  $g^z < 0$  (effectively ferromagnetic rung coupling),  $\langle \phi_s \rangle = 0$ . We can therefore replace  $\phi_s$  with its expectation value everywhere it appears in the interaction term  $H_{as}^\sigma$ . Noting that a change in sign of  $g^z$  is essentially equivalent to trading the roles of  $\sigma = +$  and  $\sigma = -$ , we confine ourselves hereafter to  $g^z > 0$ : our final conclusions on the behavior dictated by the two distinct dimerization patterns will be exchanged in the case  $g^z < 0$ .

For  $\sigma = +$ , in this semiclassical approach we obtain an effective Hamiltonian for the antisymmetric mode  $\phi_a$ ,

$$H_a^{\text{eff}} = \int dx \left\{ \frac{u_a}{2\pi} \left[ \frac{1}{K_a} (\partial_x \phi_a)^2 + K_a (\partial_x \theta_a)^2 \right] + g \cos(\sqrt{2}\theta_a) + 2g_p \cos(\sqrt{2}\phi_a) \right\}, \quad (18)$$

where the last term results from the substitution  $\sin(\sqrt{2}\phi_s) \cong \sin(\sqrt{2}\langle\phi_s\rangle) = 1$  in  $H_{as}^+$  [Eq. (16)].  $H_a^{\text{eff}}$  belongs to a class of self-dual sine-Gordon models that have known solutions [33]. This will be analyzed in detail in the next section, and it will be shown to yield a gapped, plaquette-ordered ground state. However, for  $\sigma = -$ , this naive semiclassical approximation would result in  $H_{as}^- = 0$ , since  $\cos(\sqrt{2}\phi_s) \cong \cos(\sqrt{2}\langle\phi_s\rangle) = 0$ . This would imply that the leg dimerization is completely suppressed, and by tuning  $g$  to zero one recovers a gapless Luttinger liquid state in the antisymmetric sector. Since  $H_p^\sigma = H_{as}^\sigma$  is strongly relevant, it seems improbable that it can vanish completely from the low-energy theory; rather, this is an artefact of the naive assumption  $\langle \cos(\sqrt{8}\phi_s) \rangle = -1$ . Quantum fluctuations generally induce a finite expectation value that may be different from  $-1$ , in which case  $H_{as}^-$  does not vanish. In the next section, we discuss its contribution more carefully.

### III. PHASE DIAGRAM

In what follows, we focus on the properties of the model for  $K \sim K^* \approx 1/\sqrt{2}$ , in which, as noted in the previous section, the terms responsible for the formation of leg and rung singlets are equally relevant. We derive a general theory that accounts for both the SD and CD configurations of the leg dimerization, given in terms of an effective Hamiltonian similar in form to Eq. (18). As we show below, this effective model indicates the potential formation of a ‘‘plaquette order’’ phase.

#### A. Emergence of plaquette order

As a first step in our analysis of the Hamiltonian Eq. (13), we introduce an auxiliary  $Z_2$  order-parameter field  $\hat{\tau}$  that allows us to explore the potential for spontaneous breaking of reflection symmetry across the ladder. When this occurs, this field acquires an expectation value  $\tau = \pm 1$ . As we show below, the value of  $\tau$  dictates a broken symmetry ground state where dimerization on one leg of the ladder is stronger than the other. We then define new bosonic fields via the transformation

$$\begin{aligned} \phi_{p,\tau} &= \phi_s + \tau \phi_a, & \theta_\tau &= \tau \theta_a, \\ \phi_{f,\tau} &= \sqrt{2}\phi_s, & \theta_{f,\tau} &= \frac{1}{\sqrt{2}}(\theta_s - \tau \theta_a), \end{aligned} \quad (19)$$

which preserve the canonical commutation relations

$$[\phi_{l,\tau}(x), \theta_{l',\tau}(x')] = i\pi \delta_{ll'} \text{sgn}(x - x'). \quad (20)$$

Note that from Eq. (9),  $\phi_{p,\tau}$  and  $\theta_{f,\tau}$  are simply related to the original fields  $\phi_\nu, \theta_\nu$  on the isolated legs  $\nu = 1, 2$ : for  $\tau = +$ ,  $\phi_{p,\tau} = \sqrt{2}\phi_1$  and  $\theta_{f,\tau} = \theta_2$ ; and for  $\tau = -$ , the roles of 1, 2 are interchanged. Substituting Eq. (19) in Eq. (13) and removing

the least relevant term  $\cos(\sqrt{8}\phi_a)$ , we get

$$\begin{aligned} H &= H_p^\sigma + H_f + H_{pf}^\sigma, \\ H_p^\sigma &= \frac{u_p}{2\pi} \int dx \left[ \frac{1}{K_p} (\partial_x \phi_{p,\tau})^2 + K_p (\partial_x \theta_{p,\tau})^2 \right] \\ &\quad + g \int dx \cos(\sqrt{2}\theta_{p,\tau}) + g_p (\delta_{\tau,-\sigma} + \sigma \delta_{\tau,\sigma}) \\ &\quad \times \int dx \sin(\sqrt{2}\phi_{p,\tau}), \\ H_f &= \frac{u_f}{2\pi} \int dx \left[ \frac{1}{K_f} (\partial_x \phi_f)^2 + K_f (\partial_x \theta_f)^2 \right] \\ &\quad + g^z \int dx \cos(2\phi_f), \\ H_{pf}^\sigma &= \int dx \left\{ -\frac{\sqrt{2}u_a}{K_a} \partial_x \phi_f \partial_x \phi_{p,\tau} + 2\sqrt{2}u_s K_s \partial_x \theta_f \partial_x \theta_{p,\tau} \right. \\ &\quad \left. + g_p (\delta_{\tau,\sigma} + \sigma \delta_{\tau,-\sigma}) [\sin(2\phi_f) \cos(\sqrt{2}\phi_{p,\tau}) \right. \\ &\quad \left. - \cos(2\phi_f) \sin(\sqrt{2}\phi_{p,\tau}) \right\} \end{aligned} \quad (21)$$

(for abbreviation, we removed the index  $\tau$  on the  $f$ -sector fields, where it turns out to be of no significance). Here the velocities are given by

$$\begin{aligned} u_p &= u_a \sqrt{\frac{u_a K_a + u_s K_s}{u_a K_a}} \cong \sqrt{2}u(1 - \gamma), \\ u_f &= \sqrt{u_s K_s \left( \frac{u_a}{K_a} + \frac{u_s}{K_s} \right)} \cong \sqrt{2}u \end{aligned} \quad (22)$$

and the Luttinger parameters are

$$\begin{aligned} K_p &= \sqrt{\frac{K_a(u_a K_a + u_s K_s)}{u_a}} \cong \sqrt{2}K(1 + \gamma), \\ K_f &= \sqrt{\frac{4u_s K_s^2 K_a}{u_a K_s + u_s K_a}} \cong \sqrt{2}K, \end{aligned} \quad (23)$$

where in the final approximations we neglect terms of order  $\gamma^2$ .

Next we use the fact that for  $K \cong 1/\sqrt{2}$  such that  $K_f \cong 1$ , the  $f$  sector reduces to a model of gapped free fermions. Employing Eq. (5) (with  $\phi_\nu, \theta_\nu$  replaced by  $\phi_f, \theta_f$ ), the cosine term in  $H_f$  can be reffermionized to give

$$\cos(2\phi_f) = \pi a (\psi_R^\dagger \psi_L + \psi_L^\dagger \psi_R). \quad (24)$$

This term opens a gap to excitations given by

$$\Delta = \pi a g^z \quad (25)$$

(see Appendix A for details). For low  $T \ll \Delta$ , we can simplify the interaction term  $H_{pf}^\sigma$  by a mean-field approximation. This amounts to replacing  $\cos 2\phi_f$  as well as  $\partial_x \phi_f, \partial_x \theta_f$ , and  $\sin 2\phi_f$  in  $H_{pf}^\sigma$  [Eq. (21)] by their expectation values. To

leading order in  $\Delta/u_f$ , this yields

$$\langle \sin 2\phi_f \rangle = 0, \quad \langle \partial_x \phi_f \rangle = 0, \quad \langle \partial_x \theta_f \rangle = 0, \quad (26)$$

$$O_f \equiv \langle \cos 2\phi_f \rangle \sim -\frac{|\Delta|}{u_f/a} \ln \left[ \frac{u_f/a}{|\Delta|} \right]. \quad (27)$$

Substituting back into Eq. (21), we obtain an effective model for the  $p$  sector:

$$\begin{aligned} H_p^{\sigma, \text{eff}} &= \frac{u_p}{2\pi} \int dx \left[ \frac{1}{K_p} (\partial_x \phi_{p,\tau})^2 + K_p (\partial_x \theta_{p,\tau})^2 \right] \\ &+ g \int dx \cos(\sqrt{2}\theta_{p,\tau}) \\ &+ \tilde{g}_p(\sigma, \tau) \int dx \sin(\sqrt{2}\phi_{p,\tau}), \\ \tilde{g}_p(\sigma, \tau) &\equiv (\delta_{\tau, -\sigma} + \sigma \delta_{\tau, \sigma}) g_p [1 - \sigma O_f]. \end{aligned} \quad (28)$$

The leg dimers configuration on the ladder, CD ( $\sigma = +$ ) or SD ( $\sigma = -$ ), is encoded in the effective Hamiltonian Eq. (28) by the parameter  $\tilde{g}_p(\sigma, \tau)$ . Its dependence on  $\sigma, \tau$  reflects a crucial distinction between the two patterns: first, in the CD case this effective parameter is symmetric in  $\tau$ ,  $\tilde{g}_p(+, +) = \tilde{g}_p(+, -)$ ; i.e., the Hamiltonian is identical for  $\tau = \pm$ . In contrast, the SD configuration yields  $\tilde{g}_p(-, +) = -\tilde{g}_p(-, -)$ , namely two distinct effective Hamiltonians for  $\tau = \pm$ . Second, since  $O_f < 0$  [see Eq. (27)],  $\tilde{g}_p(+, \tau)$  is always finite and obeys  $|\tilde{g}_p(+, \tau)| > |\tilde{g}_p(-, \tau)|$ . Most prominently, only in the SD case ( $\sigma = -$ ) can a gapless liquid phase be reached. This occurs for very special values of the exchange interactions where *both*  $g$  and  $\tilde{g}_p(-, \tau)$  vanish: when  $J_{\perp}^{xy} = 2J_d^{xy}$  (i.e., at the critical point of the NT model), and at the same time  $(J_{\perp}^z - 2J_d^z) \sim J_{\parallel}$  so that  $O_f \sim 1$  [34]. Then all the interaction terms vanish and we are left with a Luttinger-liquid model. For this extremely-fine-tuned point, this analysis gives a Luttinger liquid phase in the case in which the dimerization on the legs of the ladder is of the SD type [Fig. 2(b)]. This Luttinger liquid then describes gapless spinons on a single chain composed of the interlaced chains 1 and 2. It is essentially the same as the ‘‘snake chain’’ described in Ref. [24] for the isotropic Heisenberg spin ladder. We note, however, that under these conditions, another ordered ground state is likely to be favored, as will be discussed in Sec. III B.

To explore the more generic case in which  $g$  and/or  $\tilde{g}_p$  are finite, we next rescale the fields  $\tilde{\phi}_{p,\tau} = \frac{\phi_{p,\tau}}{\sqrt{2}}$ ,  $\tilde{\theta}_{p,\tau} = \sqrt{2}\theta_{p,\tau}$  and accordingly the Luttinger parameter  $\tilde{K}_p = \frac{K_p}{2}$  to obtain

$$\begin{aligned} H_{\text{eff}}^{\sigma} &= \int dx \left\{ \frac{u_p}{2\pi} \left[ \frac{1}{\tilde{K}_p} (\partial_x \tilde{\phi}_{p,\tau})^2 + \tilde{K}_p (\partial_x \tilde{\theta}_{p,\tau})^2 \right] \right. \\ &\left. + g \cos(\tilde{\theta}_{p,\tau}) + \tilde{g}_p(\sigma, \tau) \sin(2\tilde{\phi}_{p,\tau}) \right\}. \end{aligned} \quad (29)$$

For  $g > 0$ , the interaction terms  $\cos(\tilde{\theta}_{p,\tau})$ ,  $\sin(2\tilde{\phi}_{p,\tau})$  are dimerization operators, where each one creates different dimers: the  $\cos(\tilde{\theta}_{p,\tau})$  creates dimers along the rungs of the ladder, and  $\sin(2\tilde{\phi}_{p,\tau})$  creates dimers along the legs of the ladder. It is convenient to define  $\tilde{\phi}_{\tau} = \tilde{\phi}_{p,\tau} - \pi/4$ , so that  $\sin(2\tilde{\phi}_{p,\tau}) = \cos(2\tilde{\phi}_{\tau})$ , and we arrive at a self-dual sine-

Gordon model,

$$\begin{aligned} H_{\text{eff}}^{\sigma} &= \int dx \left\{ \frac{u_p}{2\pi} \left[ \frac{1}{\tilde{K}_p} (\partial_x \tilde{\phi}_{\tau})^2 + \tilde{K}_p (\partial_x \tilde{\theta}_{\tau})^2 \right] \right. \\ &\left. + g \cos(\tilde{\theta}_{\tau}) + \tilde{g}_p(\sigma, \tau) \cos(2\tilde{\phi}_{\tau}) \right\}. \end{aligned} \quad (30)$$

This is a special case of a series of models reviewed in Ref. [33]. In our case, the choice  $K \sim 1/\sqrt{2}$  dictates  $K_p \sim 1$  and hence  $\tilde{K}_p \sim 1/2$ , i.e., the quadratic part of the model is at the Heisenberg point, which is invariant under spin rotations. Then, we use the following relations:

$$\cos(\tilde{\theta}_{\tau}) \sim (-)^x \sigma_x, \quad \cos(2\tilde{\phi}_{\tau}) \sim (-)^x \sigma_z, \quad (31)$$

where the  $\sigma_a$  operators are Pauli matrices representing fictitious local spins. The resulting (fictitious) spin model is

$$\begin{aligned} H_{\text{eff}}^{\sigma} &= \sum_i [J \sigma_i \cdot \sigma_{i+1} + (-)^x \mathbf{B} \cdot \sigma_i], \\ \mathbf{B} &= \tilde{g}_p(\sigma, \tau) \hat{z} + g \hat{x}. \end{aligned} \quad (32)$$

Equation (32) describes a spin-chain model in a staggered magnetic field in the  $z$ - $x$  plane, at an angle

$$\alpha_{\tau} = \arctan(g/\tilde{g}_p(\sigma, \tau)) \quad (33)$$

from the  $\hat{z}$  direction. Now we rotate the coordinate system so that the field will be in the  $\hat{z}$  direction:

$$\hat{x}' = \cos \alpha_{\tau} \hat{x} - \sin \alpha_{\tau} \hat{z}, \quad \hat{z}' = \sin \alpha_{\tau} \hat{x} + \cos \alpha_{\tau} \hat{z}. \quad (34)$$

The  $\sigma_a$  spins are then related to the rotated spins  $\sigma'_a$  by

$$\begin{aligned} \sigma_x &= \sigma'_x \cos \alpha_{\tau} + \sigma'_z \sin \alpha_{\tau}, \\ \sigma_z &= \sigma'_z \cos \alpha_{\tau} - \sigma'_x \sin \alpha_{\tau}. \end{aligned} \quad (35)$$

After this rotation, the model is mapped onto a spin chain in a staggered magnetic field along the  $\hat{z}'$  direction, which in bosonization gives a regular sine-Gordon model with rotated fields  $\phi'_{\tau}, \theta'_{\tau}$ :

$$\begin{aligned} H_{\text{eff}}^{\sigma} &= \int dx \left\{ \frac{u'}{2\pi} \left[ \frac{1}{K'} (\partial_x \phi'_{\tau})^2 + K' (\partial_x \theta'_{\tau})^2 \right] + g'_{\tau} \cos(2\phi'_{\tau}) \right\}, \\ g'_{\tau} &\equiv \sqrt{\tilde{g}_p^2(\sigma, \tau) + g^2}, \quad u' = u_p, \quad K' = \tilde{K}_p = \frac{K_p}{2}. \end{aligned} \quad (36)$$

The  $\cos(2\phi'_{\tau})$  term opens a gap  $\Delta'$  and obtains a finite expectation value. This term is also the order parameter of this model. Recalling that  $K' \sim 1/2$ , the system is deep in the gapped phase where a semiclassical approximation is justified to evaluate  $\Delta'$ . A variational calculation (see, e.g., Ref. [32] for details) yields

$$\Delta' \sim u' \Lambda \left( \frac{K' g'_{\tau}}{u' \Lambda^2} \right)^{1/(2-K')} \quad (37)$$

with  $\Lambda \sim 1/a$ . The expectation value of the order parameter is subsequently given by

$$\langle \cos 2\phi'_{\tau} \rangle \sim - \left( \frac{g'_{\tau}}{u' \Lambda^2} \right)^{K'} \sim - \left( \frac{\Delta'}{u' \Lambda} \right)^{(2-K')K'}. \quad (38)$$

Substituting  $K' = 1/2$ , this yields

$$\Delta' \sim u' \Lambda \left( \frac{g'_\tau}{u' \Lambda^2} \right)^{2/3}, \quad \langle \cos 2\phi'_\tau \rangle \sim - \left( \frac{g'_\tau}{u' \Lambda^2} \right)^{1/2}. \quad (39)$$

Note that generically  $g'_\tau > g, \tilde{g}_P(\sigma, \tau)$  [Eq. (36)]; rather than competing with each other, the two self-dual interaction terms in Eq. (30) cooperate to form an ordered ground state that smoothly evolves upon tuning of the parameters, and there is no phase transition.

We next discuss the interpretation of the ordered state in terms of the physical spin system. Using Eqs. (31), (33), and (35), we express the order-parameter field in terms of the fields  $\tilde{\phi}_\tau$  and  $\tilde{\theta}_\tau$ :

$$\begin{aligned} \mathcal{P}_\tau &\equiv \cos(2\phi'_\tau) = \cos \alpha_\tau \cos(2\tilde{\phi}_\tau) + \sin \alpha_\tau \cos(\tilde{\theta}_\tau), \\ \cos \alpha_\tau &= \frac{\tilde{g}_P(\sigma, \tau)}{\sqrt{\tilde{g}_P^2(\sigma, \tau) + g^2}}, \quad \sin \alpha_\tau = \frac{g}{\sqrt{\tilde{g}_P^2(\sigma, \tau) + g^2}}. \end{aligned} \quad (40)$$

In both the CD ( $\sigma = +$ ) and SD ( $\sigma = -$ ) configurations, the ground state spontaneously breaks reflection symmetry across the ladder, with two distinct ground states (corresponding to  $\tau = \pm$ ) of identical energies. To understand their physical significance, recall that  $\cos(2\tilde{\phi}_\tau)$  and  $\cos(\tilde{\theta}_\tau)$  create longitudinal (on legs 1 and 2) and transverse dimers, respectively. The corresponding local dimer operators are (see Appendix B)

$$\begin{aligned} \epsilon_{l_1} &\equiv S_{j,1}^+ S_{j+1,1}^- - S_{j,1}^- S_{j+1,1}^+ \sim O_f^{\frac{1-\tau}{2}} \cos(2\tilde{\phi}_\tau), \\ \epsilon_{l_2} &\equiv S_{j,2}^+ S_{j+1,2}^- - S_{j,2}^- S_{j+1,2}^+ \sim O_f^{\frac{1+\tau}{2}} \cos(2\tilde{\phi}_\tau), \\ \epsilon_t &\equiv S_{j,1}^+ S_{j,2}^- + S_{j,1}^- S_{j,2}^+ \sim \cos(\tilde{\theta}_\tau), \end{aligned} \quad (41)$$

where  $O_f$  is given by Eq. (27). Hence Eq. (40) implies that the order parameter is an entangled superposition of longitudinal and transverse dimers on plaquettes of four spins, i.e., a resonating valence bond within the plaquette; since  $O_f < 1$ , for  $\tau = +1$  ( $\tau = -1$ ) the dimer operator on leg 1 (2) has a larger overlap with  $\mathcal{P}_\tau$ . The ground state is a crystal of such plaquettes, as illustrated in Fig. 3. Since the dimers on chains 1 and 2 have two possible configurations, CD and SD, the plaquettes are also of two distinct types: closed and open rectangular plaquettes, corresponding to the CD and SD states, respectively. The open rectangular plaquette order is relatively fragile, and under extreme conditions in which  $g'_\tau = 0$ , a gapless liquid state can be recovered. In comparison, the closed rectangle order is more robust and is lower in energy for a given strength of the exchange interactions.

The long-range order of dimers on distant plaquettes is reflected by the behavior of dimer-dimer correlation functions, which do not decay with increasing distance. We define

$$\chi_{ab}(x, t) \equiv \langle \epsilon_a(x, t) \epsilon_b(0, 0) \rangle \quad (a, b = l_1, l_2, t), \quad (42)$$

where  $\epsilon_a$  are given by Eq. (41). For  $T \ll \Delta'$  and  $x \gg \xi$ , where  $\xi = u'/\Delta'$  is the correlation length, these are approximated by constant asymptotic values:

$$\begin{aligned} \chi_{l_1 l_1}(x \gg \xi) &\cong O_f^{N_{f\nu}^\tau} \cos^2(\alpha_\tau) (\Lambda \xi)^{-2K'}, \\ \chi_{l_1 l_2}(x \gg \xi) &\cong \sin^2(\alpha_\tau) (\Lambda \xi)^{-2K'}, \\ \chi_{l_1 t}(x \gg \xi) &\cong O_f^{N_{f\nu}^\tau/2} \frac{1}{2} \sin(2\alpha_\tau) (\Lambda \xi)^{-2K'}, \end{aligned} \quad (43)$$

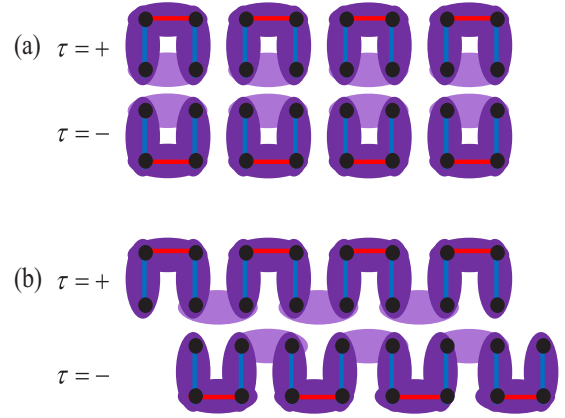


FIG. 3. (Color online) Two possible types of plaquette order on the frustrated dimerized ladder: (a) closed plaquettes corresponding to  $\sigma = +$ , (b) open plaquettes corresponding to  $\sigma = -$ . Dark purple ellipses represent strong dimers, and light purple ellipses weakened dimers. In each case, two distinct plaquette-ordered ground-state configurations emerge (corresponding to  $\tau = \pm$ ), with spontaneously broken reflection symmetry.

where  $N_{\mu\nu}^\tau$  are given by

$$N_{11}^\tau = 1 - \tau, \quad N_{22}^\tau = 1 + \tau, \quad N_{12}^\tau = N_{21}^\tau = 1 \quad (44)$$

(see details of the calculation in Appendix B). In particular, the long-range nature of  $\chi_{l,t}$ , describing the correlation between a longitudinal and a transverse dimer, indicates the entanglement between two types of dimers within a plaquette, which is a consequence of the order parameter  $\mathcal{P}_\tau$  being a superposition of longitudinal and transverse dimers [Eq. (40)]. In the limit cases in which either  $g_P$  or  $g$  vanishes,  $\chi_{l,t} = 0$  and one recovers the rung or leg dimer VBC states, respectively.

## B. Phase transition from VBC to plaquette order

The calculation presented in Sec. III B suggests that away from the NT quantum critical point, and particularly for sufficient XXZ anisotropy of the rung coupling, the competition between the transverse and longitudinal dimerization terms may give rise to an ordered state of plaquette dimers. However, since the leg dimerization term is strongly relevant, as long as  $g_P$  is still relatively large, the ground state will be dominated by the leg dimerization term, and a VBC state (as depicted in Fig. 2) will likely be favorable. This is especially notable in the case of the SD configuration ( $\sigma = -$ ), where the plaquette order is partially frustrated. When  $g$  and  $g_P$  are comparable, a first-order transition from the VBC order to the plaquette order may occur, tuned by the ratio of  $g$  and  $g_P$ . The transition line in the phase diagram, given in terms of the parameters  $g$  and  $g_P$ , can be derived from energy considerations. Toward that end, we calculate the gain in energy for each phase to form, and we compare them. The energy gain of a massive phase due to the ordering of a relevant operator is given by

$$\delta E \sim - \frac{\Delta^2}{E_0}, \quad (45)$$

where  $\Delta$  is the gap, and  $E_0 = u\Lambda$  (with  $u$  a typical velocity) is the high-energy cutoff. Similarly to the derivation of Eq. (37)

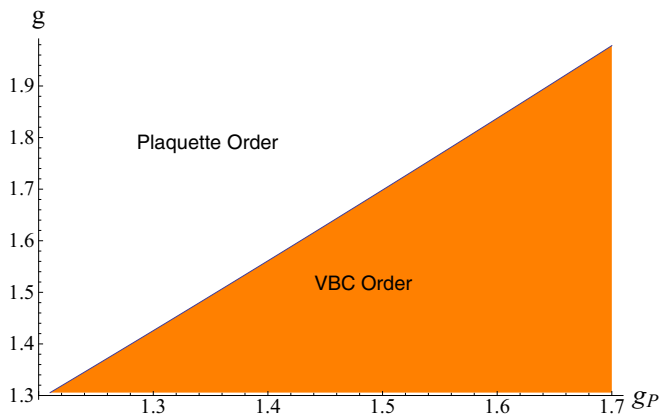


FIG. 4. (Color online)  $g$ - $g_P$  phase diagram in arbitrary units for fixed  $g^z = 1.5$ ,  $\sigma = -$ ,  $K = 1/\sqrt{2}$ ,  $\gamma = 0.1$ ,  $u = 6.15$ , and  $\Lambda = \pi$ . The phase boundary line denotes a first-order transition.

for the gap in the plaquette ordered state, we employ a variational approach to evaluate the gap opened by all relevant operators in terms of the parameters  $g_P$  and  $g^z$ . This gives

$$\begin{aligned} \Delta^z &\sim u_s \Lambda \left( \frac{K_s g^z}{u_s \Lambda^2} \right)^{\frac{1}{2-2K_s}}, \\ \Delta_P &\sim u \Lambda \left( \frac{K g_P}{u \Lambda^2} \right)^{\frac{1}{2-K}}, \end{aligned} \quad (46)$$

where  $\Delta^z$  is the gap opened by  $g^z \cos(\sqrt{8}\phi_s)$  of Eq. (13) and  $\Delta_P$  is the gap opened by the original leg dimerization term  $H_P^\sigma$  [Eq. (12)]. Using these expressions, we can calculate the gain in energy for the competing phases due to these operators. Forming a plaquette order will benefit the energy due to the gap  $\Delta'$  and the energy due to the gap  $\Delta^z$ . Forming a VBC state will benefit the energy due to the gap opened by the leg dimerization, that is, twice (counted once for each chain) the energy gain from  $\Delta_P$ . Therefore, we obtain the overall gain in energy for the competing phases to form

$$\begin{aligned} \delta E_{\text{plaq}} &= -(\Delta')^2/\Lambda u' - (\Delta^z)^2/\Lambda u_s, \\ \delta E_{\text{VBC}} &= -2(\Delta_P)^2/\Lambda u. \end{aligned} \quad (47)$$

A transition between VBC order and plaquette order occurs when  $\delta E_{\text{plaq}} = \delta E_{\text{VBC}}$ . Using Eqs. (36), (37), (46), and (47), we plot a phase diagram for the transition from VBC order to plaquette order as a function of the strength of the rung dimerization  $g$  and the leg dimerization  $g_P$  for constant  $g^z$ . The result is presented in Fig. 4.

#### IV. SUMMARY AND DISCUSSION

We studied a model for a dimerized frustrated ladder, namely a two-leg ladder version of the anisotropic NT model [8] in the presence of dimerization on the legs. Two types of dimerized patterns were considered: columnar dimers (CDs) and staggered dimers (SDs), which are, respectively, even and odd under reflection across the ladder (see Fig. 2). The effect of rung exchange interactions ( $J_\perp, J_d$ ) on the two configurations is distinct; for instance, effectively antiferromagnetic rung

coupling ( $J_\perp - 2J_d > 0$ ) strengthens the ordering due to a CD instability while it frustrates the SD configuration (and the reverse for  $J_\perp - 2J_d < 0$ ). We focus in particular on the case of an intermediate anisotropy on the legs of the ladder where the Luttinger parameter  $K \approx 1/\sqrt{2}$  [i.e.,  $J_\perp^z/J_\parallel \approx 0.6$ ; see Eq. (8)], in which the leg dimerization terms and the rung interactions are equally relevant. By mapping the resulting effective model to a spin chain in a staggered magnetic field, we found that the interplay between these interactions tends to form a ‘‘plaquette-ordered’’ phase: a crystal of resonating valence bond plaquettes where reflection symmetry across the ladder is spontaneously broken (see Fig. 3). The order parameter in this phase is a coherent superposition of longitudinal and transverse dimers, hence all types of dimer-dimer correlations are long-range.

The analysis leading to the above result relies on a mean-field approximation, justified when the rung exchange is tuned far enough from the NT quantum critical point  $J_\perp = 2J_d$ . The resulting gap to excitations is smaller in one of the dimerized configurations [e.g., for  $(J_\perp - 2J_d) > 0$  it is the SD configuration], and it can even be tuned to zero for an extreme limit of the parameters. Under these extreme conditions, one apparently expects the formation of a gapless, Luttinger liquid mode (which can be interpreted as a spin-1/2 chain meandering between the two legs of the ladder). Note that for more generic parameters, quantum fluctuations not accounted for in our low-energy approximations might also soften the gap: these introduce dynamics of the isospin auxiliary field  $\hat{\tau}$ , and consequently drive a transition of the Ising type to a liquidlike disordered phase with restored reflection symmetry. However, typically a gapless liquid state is unstable to other forms of order. In particular, for sufficiently strong dimerization (of either the CD or SD type), the Plaquette-ordered phase always gives way to the VBC state (i.e., a dimer crystal of the corresponding structure) via a *first-order* transition. A typical phase diagram is depicted in Fig. 4.

It should be noted that while the analysis presented in the previous sections was focused on a special value of the leg anisotropy ( $K = 1/\sqrt{2}$ ), allowing the exact mappings to free fermions and the Heisenberg chain in a staggered field, the conclusions are more general. The formation of a plaquette ordering essentially arises from the interplay of two highly relevant dimerization interactions, when their gap scales (as calculated for each interaction independently) are comparable. Deviations from  $K = 1/\sqrt{2}$  will thus lead to quantitative rather than qualitative corrections of our main results.

As a final remark, it is suggestive that our findings for the two-leg ladder version of the NT model are the key to understanding the behavior in physical realizations of the full-fledged 2D model such as the compound NOCuNO studied in Ref. [15]. Similarly to the CD and SD instabilities introduced in this paper, in a multichain system a variety of lattice distortions generated by the softening of certain phonon modes may occur. This is especially expected in the presence of strong spin-phonon coupling. The resulting interplay between leg and rung dimerization interactions may give rise to various ordered states involving a superposition of transverse and longitudinal dimers, such as the generalizations of the plaquette-ordered phase discussed in this paper. Moreover,

several distinct broken symmetry states with identical or comparable energy may compete. As a consequence, one generically expects the formation of domains with different ordered spin-gapped configurations. The boundaries between domains can potentially support gapless liquid of spinons. This could be manifest as a partial contribution of gapless spinons to thermodynamic coefficients, as observed in the experiment [15].

#### ACKNOWLEDGMENTS

We thank L. Balents, R. Chandra, D. Podolsky, R. Santos, and A. Tsvelik, and especially A. Vasiliev and O. Volkova for illuminating discussions. E.S. is grateful for the hospitality of the Aspen Center for Physics (NSF Grant No. 1066293) and to the Simons Foundation. This work was supported by the Israel Science Foundations (ISF) Grant No. 599/10.

#### APPENDIX A: REFORMIONIZATION OF $H_f$ AND MEAN-FIELD APPROXIMATION

Below, we derive the mapping of  $H_f$  [Eq. (21)] to gapped free fermions, and we calculate the expectation values of operators in the  $f$  sector using the reformionized version of these operators. Toward that end, we employ Eq. (5) (with  $\phi_\nu, \theta_\nu$  replaced by  $\phi_f, \theta_f$ ). For  $K_f = 1$ , the first term in Eq. (21) reduces to a kinetic energy,

$$H_f^K = -iu_f \int dx \{ \psi_R^\dagger \partial_x \psi_R - \psi_L^\dagger \partial_x \psi_L \}, \quad (\text{A1})$$

and the second term is given by Eq. (24). Transforming to momentum space, we thus obtain

$$\begin{aligned} H_f &= \sum_k u_f k (c_{R,k}^\dagger c_{R,k} - c_{L,k}^\dagger c_{L,k}) \\ &\quad + \Delta \sum_k (c_{R,k}^\dagger c_{L,k} + c_{L,k}^\dagger c_{R,k}), \\ \Delta &\equiv \pi a g^z. \end{aligned} \quad (\text{A2})$$

This Hamiltonian can be diagonalized by a Bogoliubov transformation [32]

$$c_{+,k}^\dagger = \alpha_k c_{R,k}^\dagger + \beta_k c_{L,k}^\dagger, \quad c_{-,k}^\dagger = -\beta_k c_{R,k}^\dagger + \alpha_k c_{L,k}^\dagger, \quad (\text{A3})$$

with

$$\begin{aligned} \alpha_k &= \frac{1}{\sqrt{2}} \left[ 1 + \frac{u_f k}{\sqrt{(u_f k)^2 + \Delta^2}} \right]^{1/2}, \\ \beta_k &= \frac{1}{\sqrt{2}} \left[ 1 - \frac{u_f k}{\sqrt{(u_f k)^2 + \Delta^2}} \right]^{1/2}, \end{aligned} \quad (\text{A4})$$

after which  $H_f$  becomes

$$\begin{aligned} H_f &= \sum_k \sum_{\nu=\pm} E_{\nu,k} c_{\nu,k}^\dagger c_{\nu,k}, \\ E_{\pm,k} &= \pm \sqrt{(u_f k)^2 + \Delta^2}. \end{aligned} \quad (\text{A5})$$

For low  $T \ll \Delta$ , this justifies a mean-field approximation where we replace  $\cos 2\phi_f$  as well as  $\partial_x \phi_f$ ,  $\partial_x \theta_f$  and  $\sin 2\phi_f$  in

$H_{pf}^\sigma$  by their expectation values. In terms of fermionic fields, these operators are given by

$$\begin{aligned} \sin 2\phi_f &= -i\pi a (\psi_R^\dagger \psi_L - \text{H.c.}), \\ \partial_x \phi_f &= -\pi (\psi_R^\dagger \psi_R + \psi_L^\dagger \psi_L), \\ \partial_x \theta_f &= -\pi (\psi_R^\dagger \psi_R - \psi_L^\dagger \psi_L). \end{aligned} \quad (\text{A6})$$

Fourier transforming and using Eq. (A3), we get (to leading order in  $\frac{\Delta a}{u_f}$ )

$$\begin{aligned} \langle \sin 2\phi_f \rangle &= 0, \quad \langle \partial_x \phi_f \rangle = 0, \quad \langle \partial_x \theta_f \rangle = 0, \\ O_f &\equiv \langle \cos 2\phi_f \rangle = \pi a \langle \psi_R^\dagger \psi_L + \psi_L^\dagger \psi_R \rangle \\ &= \sum_k \{ \alpha_k \beta_k (c_{+,k}^\dagger c_{+,k} - c_{-,k}^\dagger c_{-,k}) \\ &\quad + (\alpha_k^2 - \beta_k^2) (c_{+,k}^\dagger c_{-,k} + c_{-,k}^\dagger c_{+,k}) \}, \end{aligned} \quad (\text{A7})$$

which yields

$$O_f \sim -\frac{|\Delta|}{u_f/a} \ln \left[ \frac{u_f/a}{|\Delta|} \right]. \quad (\text{A8})$$

Here we have used  $\langle c_{\mu,k}^\dagger c_{\nu,k'} \rangle = \delta_{\mu\nu} \delta_{k,k'} f_{\mu,k}$  (for  $\mu, \nu = \pm$ ), with  $f_{\pm,k} = (1 + e^{E_{\pm,k}/T})^{-1}$  the Fermi distribution function, approximated by  $f_- \approx 1, f_+ \approx 0$  for  $T \ll \Delta$ . Substituting back into Eq. (21), this yields the effective Hamiltonian Eq. (28).

#### APPENDIX B: DIMER CORRELATION FUNCTIONS

We are interested in the correlations between dimers of spins in the plaquette-ordered state. Toward that end, we define the local dimerization operators (at  $x = ja$ )

$$\begin{aligned} \epsilon_{l_\nu} &= S_{j,\nu}^+ S_{j+1,\nu}^- - S_{j,\nu}^- S_{j+1,\nu}^+ = 2i \sin(2\phi_\nu) \quad (\nu = 1, 2), \\ \epsilon_t &= S_{j,1}^+ S_{j,2}^- + S_{j,1}^- S_{j,2}^+ = 2 \cos(\sqrt{2}\theta_a), \end{aligned} \quad (\text{B1})$$

where the indices  $l_{1/2}, t$  stand for longitudinal (on chain 1 or 2) and transverse dimers, respectively; note that in the expression for  $\epsilon_{l_1}$ , the site index  $j$  is even while in  $\epsilon_{l_2}$  it is even (odd) for  $\sigma = +$  ( $\sigma = -$ ). Recasting the bosonic fields  $\phi_\nu$  and  $\theta_a$  in terms of the fields defined via the transformation Eq. (19) [and subsequently in terms of  $\tilde{\phi}_\tau, \tilde{\theta}_\tau$  appearing in Eq. (30)], after using the mean-field result Eq. (26) we get

$$\begin{aligned} \sin(2\phi_1) &\sim O_f^{\frac{1-\tau}{2}} \cos(2\tilde{\phi}_\tau), \\ \sin(2\phi_2) &\sim O_f^{\frac{1+\tau}{2}} \cos(2\tilde{\phi}_\tau), \\ \cos(\sqrt{2}\theta_a) &= \cos(\tilde{\theta}_\tau). \end{aligned} \quad (\text{B2})$$

Employing the mapping to fictitious spins [Eq. (31)], a similar mapping of  $\cos(2\phi'_\tau)$  and  $\cos(\theta'_\tau)$  to  $\sigma'_x, \sigma'_z$  and the rotation Eq. (35), one obtains

$$\begin{aligned} \cos(2\tilde{\phi}_\tau) &\sim \cos(2\phi'_\tau) \cos \alpha_\tau - \cos(\theta'_\tau) \sin \alpha_\tau, \\ \cos(\tilde{\theta}_\tau) &\sim \cos(\theta'_\tau) \cos \alpha_\tau + \cos(2\phi'_\tau) \sin \alpha_\tau. \end{aligned} \quad (\text{B3})$$

The correlation functions between dimers are defined as

$$\chi_{\mu\nu}(x, t) = \langle \epsilon_\mu(x, t) \epsilon_\nu(0, 0) \rangle \quad (\mu, \nu = l_1, l_2, t). \quad (\text{B4})$$

Using Eqs. (B1)–(B3), we thus obtain expressions for  $\chi_{\mu\nu}(x, t)$  in terms of correlation functions of two types of operators:  $\cos(2\phi'_\tau)$  and  $\cos(\theta'_\tau)$ .

To calculate the correlation functions of the sine-Gordon model, we use the fact that in the gapped phase, the cosine term can be expanded around the average value of  $\phi'_\tau$ , so that  $\cos(2\phi'_\tau) \cong 2(\phi'_\tau - \pi/2)^2 - 1$ . Then, changing to a new field  $\varphi_\tau = \phi'_\tau - \pi/2$ , we arrive at a quadratic Hamiltonian for the massive field  $\varphi_\tau$ ,

$$H = \frac{u'}{2\pi} \int dx \left[ \frac{1}{K'} (\partial_x \varphi_\tau)^2 + K' (\partial_x \theta'_\tau)^2 + \frac{(\Delta')^2}{K'(u')^2} \varphi_\tau^2 \right], \quad (\text{B5})$$

with the gap  $\Delta'$  given by Eq. (37). The correlation functions of a Gaussian theory can be readily calculated using the methods shown in Appendix C of Ref. [32]. The correlations of the form  $\langle \cos(\theta'_\tau(x, t)) \cos(\theta'_\tau(0)) \rangle$  decay exponentially because due to the uncertainty principle, when  $\phi'_\tau$  is ordered,  $\theta'_\tau$  fluctuates. Therefore, at  $T \ll \Delta'$  the only contributions to  $\chi_{\mu\nu}(x, t)$  arise from the correlation function

$$C_\varphi(\mathbf{r}) \equiv \langle \cos[2\varphi_\tau(\mathbf{r}) + \pi] \cos[2\varphi_\tau(0) + \pi] \rangle \sim e^{-2K'G_\varphi(\mathbf{r})}, \quad (\text{B6})$$

where the propagator  $G_\varphi(\mathbf{r}) \equiv \langle [\varphi_\tau(\mathbf{r}) - \varphi_\tau(0)]^2 \rangle$  is given by

$$G_\varphi(\mathbf{r}) = \frac{1}{\beta\Omega} \sum_{\mathbf{q}} [1 - \cos(\mathbf{q} \cdot \mathbf{r})] \frac{2\pi u'}{\omega_n^2 + (u'k)^2 + (\Delta')^2}; \quad (\text{B7})$$

here  $\mathbf{r} = (x, u'\tau)$  with  $\tau$  the imaginary time,  $\mathbf{q} = (k, \omega_n/u')$ ,  $\beta = 1/T$ , and  $\Omega$  is the length. In the limit  $\beta, \Omega \rightarrow \infty$ , the sum

can be transformed into an integral and one obtains

$$G_\varphi(\mathbf{r}) = \frac{u'}{2\pi} \int_0^\Lambda q dq \int_0^{2\pi} d\theta_q \frac{1 - \cos[qr \cos(\theta_q)]}{(u'q)^2 + (\Delta')^2}, \quad (\text{B8})$$

where  $\theta_q$  is the angle between  $\mathbf{q}$  and  $\mathbf{r}$ ,  $q = |\mathbf{q}|$ , and  $r = |\mathbf{r}|$ . The result for  $G_\varphi(\mathbf{r})$  is

$$G_\varphi(r) = \ln(\Lambda\xi) - K_0(r/\xi), \quad \xi \equiv u'/\Delta', \quad (\text{B9})$$

where  $K_0(z)$  is the modified Bessel function. Using the asymptotic and series expansions of  $K_0(z)$  for large and small arguments,

$$K_0(z \gg 1) \approx \sqrt{\frac{\pi}{z}} e^{-z}, \quad K_0(z \ll 1) \approx -\ln(z), \quad (\text{B10})$$

we obtain a result for  $C_\varphi$  [Eq. (B6)] in the following two limits:

$$C_\varphi(r \ll \xi) \cong (r\Lambda)^{-2K'}, \quad C_\varphi(r \gg \xi) \cong (\Lambda\xi)^{-2K'}. \quad (\text{B11})$$

Finally, employing Eqs. (B1)–(B3), this yields the correlation functions [Eq. (B4)] in the limit  $r \gg \xi$ :

$$\begin{aligned} \chi_{l_\mu l_\nu}(x \gg \xi) &\cong O_f^{N_{\mu\nu}^\tau} \cos^2(\alpha_\tau) (\Lambda\xi)^{-2K'}, \\ \chi_{ll}(x \gg \xi) &\cong \sin^2(\alpha_\tau) (\Lambda\xi)^{-2K'}, \\ \chi_{l_\nu l}(x \gg \xi) &\cong O_f^{N_{\nu\nu}^\tau/2} \frac{1}{2} \sin(2\alpha_\tau) (\Lambda\xi)^{-2K'}, \end{aligned} \quad (\text{B12})$$

where  $N_{\mu\nu}^\tau$  are given by

$$N_{11}^\tau = 1 - \tau, \quad N_{22}^\tau = 1 + \tau, \quad N_{12}^\tau = N_{21}^\tau = 1. \quad (\text{B13})$$

- 
- [1] H. Bethe, *Z. Phys.* **71**, 205 (1931).  
[2] L. Balents, *Nature (London)* **464**, 199 (2010).  
[3] E. Dagotto, J. Riera, and D. Scalapino, *Phys. Rev. B* **45**, 5744 (1992).  
[4] T. M. Rice, S. Gopalan, and M. Sigrist, *Europhys. Lett.* **23**, 445 (1993).  
[5] T. M. Rice, S. Gopalan, and M. Sigrist, *Physica B* **199**, 378 (1994).  
[6] H. J. Schulz, *Phys. Rev. Lett.* **77**, 2790 (1996).  
[7] F. H. L. Essler, A. M. Tsvelik, and G. Delfino, *Phys. Rev. B* **56**, 11001 (1997).  
[8] A. A. Nersisyan and A. M. Tsvelik, *Phys. Rev. B* **67**, 024422 (2003).  
[9] P. W. Anderson, *Mater. Res. Bull.* **8**, 153 (1973).  
[10] A. M. Tsvelik, *Phys. Rev. B* **70**, 134412 (2004).  
[11] S. Moukouri, *Phys. Rev. B* **70**, 014403 (2004).  
[12] O. A. Starykh and L. Balents, *Phys. Rev. Lett.* **93**, 127202 (2004).  
[13] T. Hikihara and O. A. Starykh, *Phys. Rev. B* **81**, 064432 (2010).  
[14] P. Sindzingre, *Phys. Rev. B* **69**, 094418 (2004).  
[15] O. Volkova, I. Morozov, V. Shutov, E. Lapsheva, P. Sindzingre, O. Cépas, M. Yehia, V. Kataev, R. Klingeler, B. Büchner, and A. Vasiliev, *Phys. Rev. B* **82**, 054413 (2010).  
[16] V. Gnezdilov, P. Lemmens, Yu. G. Pashkevich, D. Wulferding, I. V. Morozov, O. S. Volkova, and A. Vasiliev, *Phys. Rev. B* **85**, 214403 (2012).  
[17] E. Shimshoni, N. Andrei, and A. Rosch, *Phys. Rev. B* **68**, 104401 (2003).  
[18] O. Shlagman and E. Shimshoni, *Phys. Rev. B* **86**, 075442 (2012).  
[19] F. D. M. Haldane, *Phys. Lett. A* **93**, 464 (1983); *Phys. Rev. Lett.* **50**, 1153 (1983).  
[20] I. Affleck, *Nucl. Phys. B* **265**, 409 (1986).  
[21] I. Affleck and F. D. M. Haldane, *Phys. Rev. B* **36**, 5291 (1987).  
[22] M. A. Martin-Delgado, R. Shankar, and G. Sierra, *Phys. Rev. Lett.* **77**, 3443 (1996).  
[23] M. A. Martin-Delgado, J. Dukelsky, and G. Sierra, *Phys. Lett. A* **250**, 430 (1998).  
[24] D. C. Cabra and M. D. Grynberg, *Phys. Rev. Lett.* **82**, 1768 (1999).  
[25] Y.-J. Wang and A. A. Nersisyan, *Nucl. Phys. B* **583**, 671 (2000).  
[26] S. T. Carr, A. O. Gogolin, and A. A. Nersisyan, *Phys. Rev. B* **76**, 245121 (2007).  
[27] J. Almeida, M. A. Martin-Delgado, and G. Sierra, *Phys. Rev. B* **77**, 094415 (2008).  
[28] G. Y. Chitov, B. W. Ramakko, and M. Azzouz, *Phys. Rev. B* **77**, 224433 (2008).  
[29] S. J. Gibson, R. Meyer, and G. Y. Chitov, *Phys. Rev. B* **83**, 104423 (2011).  
[30] D. G. Shelton, A. A. Nersisyan, and A. M. Tsvelik, *Phys. Rev. B* **53**, 8521 (1996).

- [31] A. O. Gogolin, A. A. Nersesyan, and A. M. Tsvelik, *Bosonization and Strongly Correlated System* (Cambridge University Press, Cambridge, England, 1998).
- [32] T. Giamarchi, *Quantum Physics in One Dimension* (Oxford University Press, Oxford, 2004).
- [33] P. Lecheminant, A. O. Gogolin, and A. Nersesyan, *Nucl. Phys. B* **639**, 502 (2002).
- [34] Note that in this limit, our derivation does not strictly apply since the underlying assumption of weak rung-coupling approximation breaks down.